ELSEVIER

Journal of Nuclear Materials 290–293 (2001) 1009–1012

journal of nuclear materials

www.elsevier.nl/locate/jnucmat

Edge transport barrier formation and ELM phenomenology in the W7-AS stellarator

P. Grigull *, M. Hirsch, J. Baldzuhn, H. Ehmler, F. Gadelmeier, L. Giannone, H.-J. Hartfuss, D. Hildebrandt, R. Jaenicke, J. Kisslinger, R. Koenig, K. McCormick, F. Wagner, A. Weller, Ch. Wendland, W7-AS Team

Max-Planck-Institut für Plasmaphysik, EURATOM Association, Boltzmannstrasse 2, D-85748 Garching, Germany

Abstract

In NBI discharges with density ramps in W7-AS, the quiescent H-mode is restricted to the same ranges of the edge rotational transform as in ECRH discharges and occurs above threshold densities $\geqslant 10^{20}$ m^{-3} which increase with heating power. Higher power needs higher density for stabilization. The approach to the quiescent H-mode often occurs, with increasing density and decreasing power flow through the edge, from grassy through dithering states to bursts of ELMs and, in a few cases, quasi-periodic ELMs. This goes parallel with increasing radial gradients of the plasma pressure and E-field at the edge. Higher heating power reduces in particular the T_i gradients and hence the E-field gradients, which effect can be compensated by higher density. The correlations found are fairly consistent when an $E \times B$ flow shear decorrelation of the turbulent transport is assumed.

Keywords: H-mode; W7-AS

1. Introduction

A number of studies on the H-mode in W7-AS ($R = 2$ m, $a \leqslant 0.18$ m) have yielded evidence that the H-mode-related phenomena show strong similarities to those observed in tokamaks [1–6]. The H-mode existence boundaries, on the other hand, seem to exhibit remarkable peculiarities compared with tokamaks, a result which should not be surprising in view of the highly different magnetic field topologies and, hence, different stability and transport properties. One of these peculiarities is that the ELM-free H-mode (H*) in W7-AS is restricted to relatively narrow windows of the edge rotational transform ι_a [1–3], whereas H-mode-related dynamic phenomena ('grassy', dithering and/or ELMy scenarios) were found in much broader ι_a ranges. Furthermore, data from ECR-heated discharges indicate the existence of a threshold density for the H*-mode increasing with power, $\bar{n}_e^{thr} \propto P$, and not the reverse, $P^{thr} \propto \bar{n}_e$, as is known from tokamaks. If, at a given density, the heating power is increased, the H*-mode vanishes. In Ref. [4] it was conjectured that this behaviour may be typical of electron-heated plasmas with relatively weak coupling to the ions. This would imply that the H-mode in high-density, NBI-heated discharges behaves differently. The present analysis focuses on this issue. It continues recent studies on net current-free NBI discharges [5,6] by presenting further details of the H-mode phenomenology and relating them as far as a available to edge plasma parameters.

2. Results and discussion

The study comprises NBI-heated discharges with density ramps at constant heating power (0.4 MW) and varied rotational transform ($\iota_a = 0.47$–0.57), and at constant rotational transform ($\iota_a = 0.558$) and varied heating power (0.4–1.6 MW). The densities were ramped up to the final values within about 0.5–0.6 s. The

* Corresponding author. Tel.: +49-89 3299 1619.
E-mail address: grigull@ipp.mpg.de (P. Grigull).

0022-3115/01/$ - see front matter
PII: S0022-3115(00)00659-0

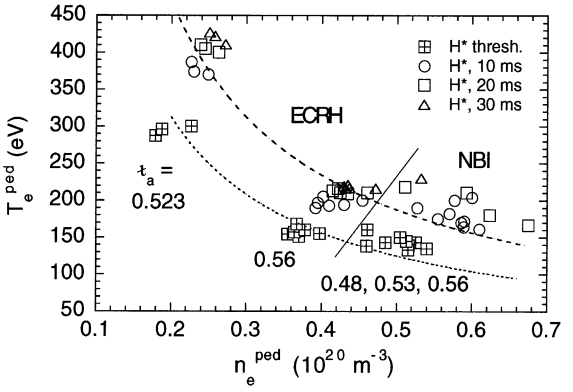

Fig. 1. Electron temperatures T_e^{ped} versus densities n_e^{ped} measured 2 cm inside the separatrix (from ECE and Li beam, respectively) immediately before, and 10, 20 and 30 ms after the transition to the H*-mode. Density ramps with 0.4 MW ECRH or NBI. Lines indicate $n_e^{ped} T_e^{ped} = \text{const}$.

quiescent H-mode typically occurs above threshold densities $\bar{n}_e^{thr} \geqslant 10^{20}$ m^{-3} within the same ι_a windows already known from ECR heated discharges (ι_a around 0.48, 0.53 and 0.56). There is strong indication that these windows correspond to minimum neoclassical viscous damping of the plasma poloidal rotation [6,7]. The $\bar{n}_e^{thr}$ values are (a factor up to two) higher than for ECR-heated discharges at the same heating power. Outside the ι_a ranges mentioned, the discharges showed grassy, dithering or ELMy phases, but transitions to the H*-mode were not observed.

The transitions to the H*-mode show well-known signatures (see, e.g., Fig. 3 in [5]): the gradients of the electron temperature T_e, ion temperature T_i and density n_e steepen (starting at the outermost edge) leading to decreased downstream T_e values and particle fluxes onto the targets. The H_α signal (from a limiter) drops sharply and changes, in this case, from grassy to quiescent. Concurrently, a negative radial electric field E_r builds up, which is consistent with the hypothesis of transport barrier formation due to sheared $E \times B$ plasma flow. T_e and n_e radial profiles indicate that the transport barrier extends 3–4 cm inside the separatrix with pivot points slightly inside but close to the separatrix. The gain in energy confinement time is by up to a factor of 1.6. Pedestal electron temperatures and densities immediately before and after the transition to the H*-mode (indicated by the drop in the H_α intensity) and $T_e n_e$ isobars for orientation are shown in Fig. 1. For ECRH discharges, the threshold values depend on the ι_a window, whereas NBI discharges at the same heating power generally show high-n_e^{ped}, low-T_e^{ped} thresholds.

Unlike in the example referred to above, often the discharges approach the H*-mode more continuously, Fig. 2. At fixed NBI power and with increasing density, the initial grassy phase (e.g., at $t < 333$ ms in Fig. 2) is

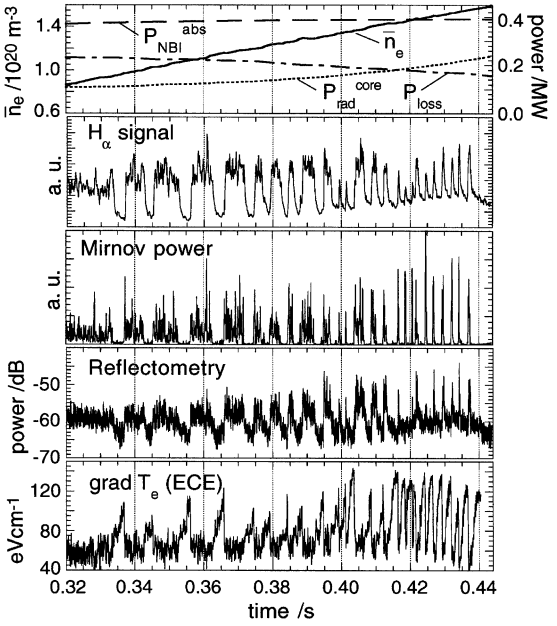

Fig. 2. Typical evolution of edge plasma characteristics preceding a transition to the H*-mode. ∇T_e was measured at $a - 1$ cm. ECE signals are running into cut-off at 0.44 s. The approach to the H*-mode levels proceeds with increasing density and decreasing power flow P_{loss} through the edge.

typically followed by a grassy scenario with intermittent, short, quiescent phases (dithering, $333 < t < 400$ ms) with increasing repetition rate, which then develops to the H*-mode via bursts of ELMs or (in a few cases) a sequence of well-separated, quasiperiodic ELMs. The ELMs are characterized by bursts of fluctuations in density and magnetic field. Reflectometry measures the density perturbation first 3–4 cm inside the separatrix and indicates radial outward propagation of the order of 1 km/s. During the ELMs, Mirnov spectra show dominating frequency bands (up to 400 kHz) depending on the discharge conditions. Often, quasi-coherent precursor activity is observed which starts about 50 μs before the transport increases [2]. The flattening of the T_e and n_e radial profiles at the edge (breakdown of the transport barrier) has pivot points typically 1–3 cm inside the separatrix (from ECE, reflectometry and Li beam). The events during grassy phases show phenomenological similarities to single ELMs. They appear as irregular spikes (averaged repetition rates about 2 kHz) in the H_α signal and – well correlated – in the ECE temperatures at different radii in the edge region. The latter indicate edge-localized flattening of the T_e radial profiles with pivot point scattering around those of single ELMs. At the discharge conditions studied in this analysis, the Mirnov spectra ($\geqslant 30$ kHz) during both grassy spikes and single ELMs show a broad band activity (up to about 200 kHz) with several peaks centered around a

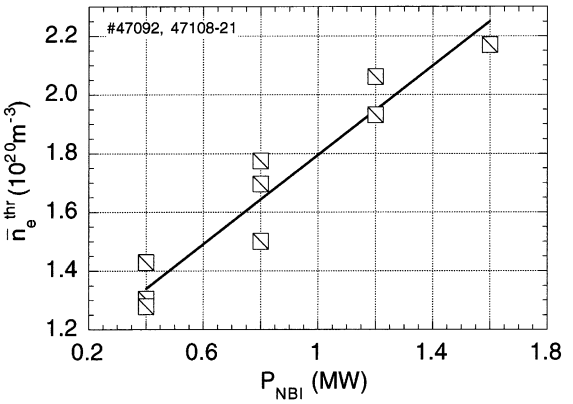

Fig. 3. Threshold densities $\bar{n}_e^{thr}$ for the transition to the H*-mode as a function of the applied heating power for NBI discharges ($\iota_a = 0.558$) with density ramps. The NBI power was varied from discharge to discharge.

frequency of about 140 kHz. Single ELMs show the tendency of these peaks to concentrate at a somewhat narrower frequency range (≈120–160 kHz) than for grassy events, but this difference is not well reproducible and seems to be not specific. As shown in, for example, Fig. 2(a), the net power flow through the edge $P_{loss} = P_{NBI}^{abs} - P_{rad}^{core} - dW/dt$ (with p_{NBI}^{abs} being the absorbed NBI power, P_{rad}^{core} the total radiation from the core, and W the stored energy) decreases with increasing density due to enhanced radiation from the core, which is typical of these high-density NBI discharges. This means that the stabilization of the transport-enhancing events, and hence the approach to the H*-mode, generally proceeds with increasing $\bar{n}_e$ and decreasing P_{loss}.

In keeping with this latter statement, higher NBI power shifts $\bar{n}_e^{thr}$ for the transition to the H*-mode to higher values, $\bar{n}_e^{thr} \propto P_{NBI}$. Fig. 3 shows $\bar{n}_e^{thr}$ values for NBI power scans (from shot to shot) with density ramps at $\iota_a = 0.558$. This result basically recovers the results from ECR-heated discharges and refutes the assumption mentioned in the introduction that this property could be typical of electron-heated discharges only. As will be shown, the reason for this common behaviour of ECR and NBI-heated discharges seems to be the dependence of the ion temperature and its gradient at the edge on the density and heating power, which shows a similar tendency in both cases.

Fig. 4 relates the impact of the heating power on the development towards the H*-mode to edge parameters for typical examples. Fig. 4(a) plots P_{loss} versus $\bar{n}_e$ for one to four applied NBI sources, each with 0.4 MW. The approach to the H*-mode is indicated by the factor f_s, which relates the total duration of the quiescent phases between ELMS or bursts of ELMs within a certain time interval (20 ms) to the length of the interval. A value of $f_s \approx 0.2$ indicates the onset of strong dithering; in-

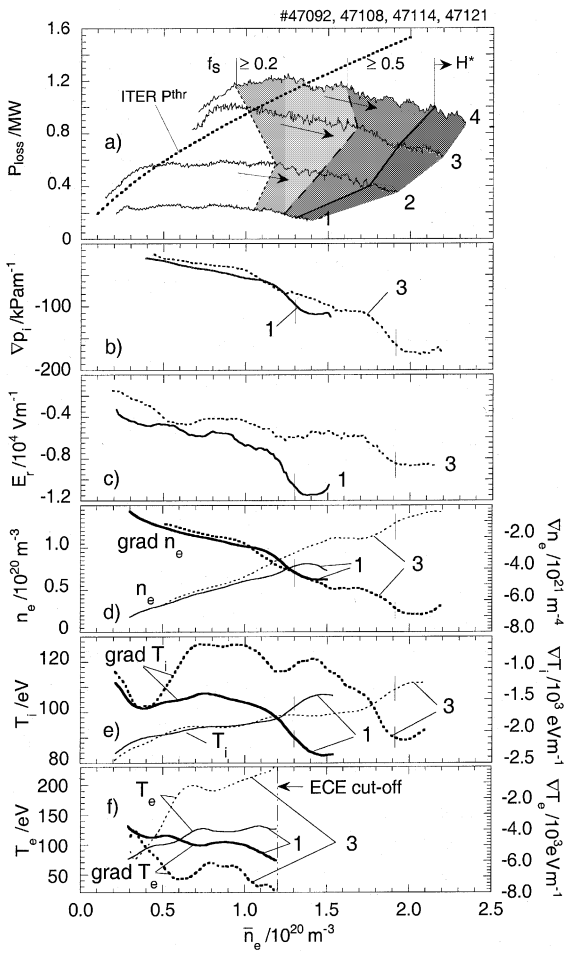

Fig. 4. Edge plasma parameters versus $\bar{n}_e$ for an NBI power scan at $\iota_a = 0.558$ with density ramps. Numbers 1–4 indicate the number of NBI sources applied, each with a constant power of 0.4 MW. Increasing stabilization of dynamic phenomena preceding the transition to the H*-mode are indicated by factors f_s (see text) and increasing shading in (a). The ITER LH power threshold scaling [8] with W7-AS parameters (B, plasma surface S) is shown for comparison. Thin vertical bars in (b)–(e) indicate the transition to the H*-mode according to (a). The data in (b)–(f) were measured at an effective plasma radius of 12.5 cm ($a - 1.5$ cm). Since the time resolution (3.5 ms) is insufficient to resolve the full dynamics, smoothed curves through the data are shown.

creasing values above ≈0.5 indicate the development from bursts of ELMs to quasi-periodic ELMs. The figure confirms that increasing power needs increasing density for stabilization of the transport-enhancing events. It shows that, within the parameter range studied, the H*-mode occurs at a given density *below*, and not above, a certain power threshold as in tokamaks [8]. The approach to the H*-mode with increasing density goes parallel with increasing ion pressure gradients ∇p_i

and increasing negative radial electric fields E_r and hence ∇E_r at the edge (about 1.5 cm inside the separatrix, Figs. 4(b) and (c)).

The data were obtained from Li beam and BIV line emission spectroscopy [9] with a time resolution of 3.5 ms. Fig. 4(c) shows that higher power leads, at the same density, to a reduction of the measured negative E_r-field. This behaviour can be primarily related to the ion temperature gradients, Fig. 4(e). For an explanation, the ambipolarity constraint is solved by using the neoclassical definitions of the particle fluxes. Experimentally, we find the ion-root solution with negative E_r-field in the gradient region, which means that the ion fluxes become very small, $\Gamma_i^{neo} \approx 0$. This provides a linear relation between E_r and ∇T_i [10]:

$$\left(\frac{D_{12}}{D_{11}}\frac{\nabla T_i}{T_i}+\frac{\nabla n_i}{n_i}\right)T_i = eE_r.$$

The ratio D_{12}/D_{11} of the transport coefficients is found to be nearly constant. Higher power increases T_e and ∇T_e (from ECE, Fig. 4(f)), but reduces ∇T_i and hence the negative E_r-fields as measured. This effect can then be compensated by higher density leading to higher ∇T_i and $\nabla n_i/n_i$ values ($n_i = n_e$ assumed). Anomalous particle fluxes seem to be intrinsically ambipolar in W7-AS and do not contribute to the E_r-field formation at the edge. Measured E_r values can generally be well reproduced from thermal, neoclassical fluxes [11].

The approach to the H*-mode, expressed by the 'stabilization factor' f_s, is correlated with the development of the E_r-field gradients, Fig. 5, which is consistent with the hypothesis of a reduction of the turbulent transport by $E \times B$ flow shear. Fig. 5 and a comparison of Figs. 4(b) and (c) further indicate that higher pressure gradients at the edge – at higher heating power – lead to transitions to the H*-mode already at smaller E_r-field and hence E_r-field gradients, which means that the combination of both high negative E_r-field- and high plasma pressure gradients at the edge seems to favor the transition.

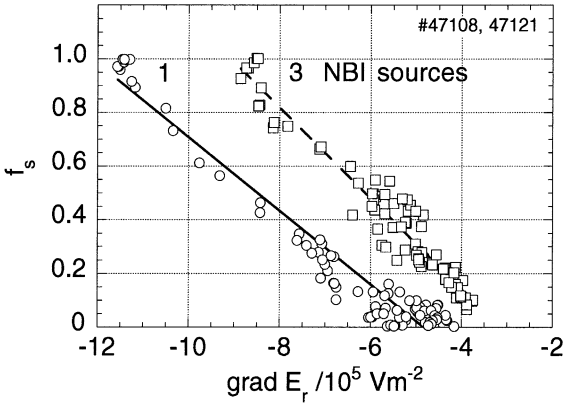

Fig. 5. 'Stabilization factors' f_s (see text) versus ∇E_r at the edge ($a - 1.5$ cm) for the discharges shown in Figs. 4(b)–(f).

3. Summary and conclusions

Transitions to the H-mode were studied in NBI-heated discharges with density ramps at constant heating power (0.4 MW) and varied rotational transform ($\iota_a = 0.47$–0.57), and at constant rotational transform ($\iota_a = 0.558$) and varied heating power (0.4–1.6 MW). The quiescent H-mode occurs above threshold densities $\geqslant 10^{20}$ m^{-3}, which increase with the power flow through the edge, and is restricted to certain ι_a windows which recover the ranges already found with ECRH. The approach to the quiescent phase generally occurs, with increasing density and decreasing power flow through the edge, from grassy through dithering states to bursts of ELMs and, in a few cases, quasi-periodic ELMs. The transition from dithering to bursts of ELMs seems to be quasi-continuous; the data do not show significant differences. The approach to the quiescent state with increasing density goes parallel with increasing plasma pressure and radial E-field gradients at the edge. At a given density, higher heating power increases T_e and ∇T_e, but reduces ∇T_i and hence the E-field gradients, which effect can then be compensated by higher density. On the assumption that the turbulent transport is reduced by $E \times B$ flow shear, the observed correlations are fairly consistent.

References

[1] F. Wagner et al., Plasma Phys. Control. Fus. 36 (1994) A61.
[2] M. Hirsch et al., in: Proceedings of the 16th IAEA Conference on Plasma Physics and Controlled Nuclear Fusion Research, vol. 2, Montreal, 1996, p. 315.
[3] M. Hirsch et al., Plasma Phys. Control. Fus. 40 (1998) 631.
[4] F. Wagner et al., Trans. Fus. Technol. 27 (1995) 32.
[5] P. Grigull et al., in: Proceedings of the 26th EPS Conference on Controlled Fusion and Plasma Physics, vol. 23J, Maastricht, 1999, p. 1473.
[6] M. Hirsch et al., Plasma Phys. Control. Fus. 42 (2000) A231.
[7] H. Wobig, J. Kisslinger, Report IPP III/250, Institut für Plasmaphysik, EURATOM Association, Garching, 1999.
[8] ITER Physics Basis Group, Nucl. Fus. 39(12) (1999) 2195.
[9] J. Baldzuhn, W. Ohlendorf, W7-AS Team, Rev. Sci. Instrum. 68(1) (1997) 1020.
[10] H. Maassberg et al., Phys. Fluids B 5 (1993) 3627.
[11] J. Baldzuhn, M. Kick, H. Maassberg, W7-AS Team, Plasma Phys. Control. Fus. 40 (1998) 967.